Chalcogenide Letters Vol. 18, No. 3, March 2021, p. 123 - 127

MASS ATTENUATION COEFFICIENT OF $[(TeO_2)_{0.7}(B_2O_3)_{0.3}]_{1-x}(BaO)_x$ GLASS FOR ENERGY OF 1 KeV – 100 GeV

A. AZURAIDA[a,*], M. K. HALIMAH[b], M. ISHAK[c], N. R. FADHILAH[a], A. NORHAYATI[c], N. AHMAD[a]

[a]*Physics Department, Centre for Defence Foundation Studies, Universiti Pertahanan Nasional Malaysia, 57000 Sungai Besi, Kuala Lumpur, Malaysia*

[b]*Physics Department, Faculty of Science, Universiti Putra Malaysia, 43400 UPM Serdang, Selangor, Malaysia*

[c]*Malaysia Nuclear Agency, 43000, Bangi, Kajang, Selangor, Malaysia*

The gamma shielding parameters of $[(TeO_2)_{0.7}(B_2O_3)_{0.3}]_{1-x}(BaO)_x$ glass system in terms of attenuation coefficient, effective atomic number and electron density have been obtained theoretically by WinXCOM programme. The mass attenuation coefficient of all glasses increases with increasing amount of barium oxide, BaO. In present work, the highest composition of BaO in glass system (x = 0.25 mol %) give the highest value of mass attenuation coefficient, μ_m. Another shielding parameter such as effective atomic number (Z_{eff}) and electron density (N_e) estimated using WinXCOM programme are depending to the barium composition and photon energy.

(Received December 2, 2020; Accepted March 9, 2021)

Keywords: Barium, Boro-tellurite, Mass attenuation coefficient

1. Introduction

Lead-shielding glass has been widely used to reduce ionizing radiation in medical x-ray imaging systems, particularly on windows. The use of lead however has led to a number of adverse effects including damage to the kidney and brain, miscarriage, and disturbance of the nervous system. The International Agency for Research on Cancer (IARC) and The Department of Health and Human Services (DHHS) have found that lead and its compounds cause environmental toxicity and are potentially carcinogenic to humans. Due to the effects mentioned above, barium has a significant role in replacement of lead for the development of radiation shielding material. The introduction of barium in lead-free glass can improve radiation shielding properties [1]. Saudi et al. (2019) [2] proved that barium-borate glass are good candidate as a protective shield against nuclear radiations. Previous work also found that barium borate glass system has superior shielding capacity against gamma rays and fast neutrons as compared with different conventional shielding material and commercial glasses [3].

The aim of present work is to evaluate the theoretical shielding parameter of $[(TeO_2)_{0.7}(B_2O_3)_{0.3}]_{1-x}(BaO)_x$ glass system using WinXCom program at energy of 1 keV – 100 GeV. In this study, boro-tellurite was selected as the base glass due to its specific characteristics, such as high transparency and good gamma shielding properties when combined with heavy metal oxides. The addition of barium oxide in boro-tellurite-based glass is expected to improve the shielding parameter for the gamma radiation. Current work aims to synthesize transparent radiation shielding glasses modified with barium element. This paper will report the effects of barium in a boro-tellurite glass system which concentrates on two properties: (i) physical and structural properties, and (ii) gamma radiation shielding properties. Boro-tellurite was chosen as a base glass in this research because of its unique characteristics such as high transparency, good gamma shielding properties and high thermal resistance when added with heavy metal oxides [8]. It is expected that the addition of barium oxide in boro-tellurite glass would increase the glass density and improve the gamma radiation shielding properties.

* Corresponding author: azuraida@upnm.edu.my

https://doi.org/10.15251/CL.2021.183.123

2. Theoretical calculation for shielding parameter

The glass system with chemical composition of $[(TeO_2)_{0.7}(B_2O_3)_{0.3}]_{1-x}(BaO)_x$ (where x = 0, 0.05, 0.10, 0.15, 0.20 and 0.25 mol%) were studied in this work. Based on the mixture rule, the theoretical values of the mass attenuation coefficients of this glass system were evaluated by WinXCom programme [6]:

$$\mu_m = \sum_i w_i(\mu_m)_i \tag{1}$$

where w_i is the weight fraction of element and $(\mu_m)_i$ is the mass attenuation coefficient for individual element (Te, B, Ba and O). The total atomic cross-section $(\sigma_{t,a})$ can be determined from the value of the mass attenuation coefficients obtained using the following relation.

$$\sigma_{t,a} = \frac{\mu_m}{N_A \sum_i^n (w_i/A_i)} \tag{2}$$

where N_A is Avogadro's number, A_i is atomic weight of constituent element. The total electronic cross-section $(\sigma_{t,el})$ for the element is also expressed by the following formula:

$$\sigma_{t,el} = \frac{1}{N_A}\sum_i^n \frac{f_i A_i}{Z_i}(\mu_m)_i \tag{3}$$

where f_i is the number of atoms of element i relative to the total number of atoms of all elements in glass system and Z_i is the atomic number of the ith element. The total atomic cross-section and the total electronic cross-section are related to the effective atomic number (Z_{eff}) of the glass material by the following relation [7]:

$$Z_{eff} = \frac{\sigma_{t,a}}{\sigma_{t,el}} = \frac{\sum f_i A_i (\mu/\rho)_i}{\sum f_j (A_j/Z_j)(\mu/\rho)_j} \tag{4}$$

The electron density can be defined as the number of electrons per unit mass, and it can be mathematically written as follows:

$$N_{el} = \frac{\mu_m}{\sigma_{t,el}} \tag{5}$$

3. Results and discussion

The theoretical values of mass attenuation coefficients (μ_m), effective atomic number (Z_{eff}), and electron density (N_{el}) of $[(TeO_2)_{0.7}(B_2O_3)_{0.3}]_{1-x}(BaO)_x$ glass system are calculated for the energy range from 1 keV to 100 GeV. These theoretical values are calculated by using WinXcom program. The prediction of theoretical shielding parameters are also found for polymer [8], concrete [9], alloy [10] and compound [11,12].

The chemical composition of $[(TeO_2)_{0.7}(B_2O_3)_{0.3}]_{1-x}(BaO)_x$ glass system with different % mol are listed in Table 1. The calculated value of μ_m for $[(TeO_2)_{0.7}(B_2O_3)_{0.3}]_{1-x}(BaO)_x$ glass system in range of 1 keV to 100 GeV is illustrated in graph at Fig. 1. In general, it can be seen that the addition of barium oxide in $[(TeO_2)_{0.7}(B_2O_3)_{0.3}]_{1-x}(BaO)_x$ glass system causes an increase in mass attenuation coefficient, μ_m. The decrement and increment of one μ_m line with other μ_m lines in the graph is influenced by photon energy, glass density [13] and chemical composition in glasses.

Table 1. Glass code with % mol of BaO content.

Glass Code	BaO, % mol	Glass Composition
BTe	0	$[(TeO_2)_{0.7}(B_2O_3)_{0.3}]$
5BaBTe	0.05	$[(TeO_2)_{0.7}(B_2O_3)_{0.3}]_{0.95}(BaO)_{0.05}$
10BaBTe	0.10	$[(TeO_2)_{0.7}(B_2O_3)_{0.3}]_{0.90}(BaO)_{0.10}$
15BaBTe	0.15	$[(TeO_2)_{0.7}(B_2O_3)_{0.3}]_{0.85}(BaO)_{0.15}$
20BaBTe	0.20	$[(TeO_2)_{0.7}(B_2O_3)_{0.3}]_{0.80}(BaO)_{0.20}$
25BaBTe	0.25	$[(TeO_2)_{0.7}(B_2O_3)_{0.3}]_{0.75}(BaO)_{0.25}$

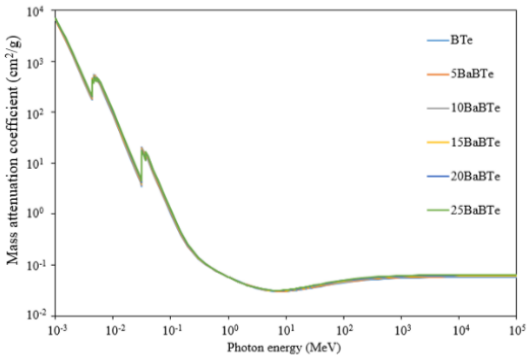

Fig. 1. The mass attenuation coefficient, μ_m for different photon energies of $[(TeO_2)_{0.7}(B_2O_3)_{0.3}]_{1-x}(BaO)_x$ glass systems.

The mass attenuation coefficient of the glass system for energy < 1 MeV dropped quickly due to prevalence of photoelectric interaction. The zigzags curve (sharp discontinuities) appears in Fig. 1 which also name as "absorption edge" is maybe due to binding energy of electrons from atom's bound shells. The sharp discontinuities exist around 0.09 MeV correspond to the absorption K-edge of bismuth. Another sharp discontinuities peak appears in graph maybe due to the interaction of photon with electron from L, M and/or N shell in energetically impossible and therefore the probability drops abruptly [5].

The μ_m values of present glasses decrease slowly with increasing of energy (at intermediate energy range of 1 MeV < E < 7 MeV). Then, it value became nearly zero when the energy almost at 7 MeV. In this energy level, the Compton Scattering mechanism and photoelectric interaction take place. Then, for the energy E > 11 MeV, the mass attenuation coefficient, μ_m of the glasses is increase moderately until the energy reaches 30 GeV and then the μ_m value are nearly constant when the energy become 100 GeV. This is corresponding to the pair production cross section, which is directly proportional to log E [14]. The pattern of graph shown in Fig. 1 are not influence by atomic number, Z. The same graph pattern also shown by previous work for glasses with Bi_2O_3 content [5]. This Bi_2O_3 glass content have higher density compare to present work (glasses with BaO). However, the pattern of the graph for mass attenuation coefficient against photon energy for both works are same. This similar behavior also shown in several works before using different glass based [15-17].

The effective atomic number, Z_{eff} of $[(TeO_2)_{0.7}(B_2O_3)_{0.3}]_{1-x}(BaO)_x$ glass system is shown in Fig. 2. The graphs vary with gamma ray energies ranging from 1 keV to 100 GeV and the values range between 31.55 and 54.27. The figure shows that the values of Z_{eff} increased in the energy region E < 10 KeV and decreased as the energy increased to 1 MeV. The Z_{eff} graph for all glass compositions changes drastically in this energy region (E < 1 MeV). The drastic changes are due to the Ba (K-, L- and M-edge) and Te (K-, L- and M-edge) absorption edges. However, the small absorption edge (K-, L- and M edge) shown for BTe glass, was seen only from Te element. It is widely known that chemical effects are appreciable only near the absorption edges [18].

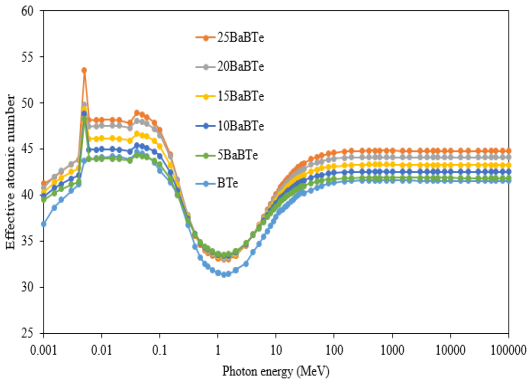

Fig. 2. Effective atomic number for different photon energies of $[(TeO_2)_{0.7}(B_2O_3)_{0.3}]_{1-x}(BaO)_x$ *glasses.*

The Z_{eff} values shows a slow increase as the gamma energy increases to 18 MeV. The Compton scattering mechanism is dominant and it is found that the interaction cross section is directly proportional to the Z atomic number [15]. Moreover, the value of Z_{eff} value becomes constant for energy above 100 MeV. This behavior is attributed to the dominance of pair production.

Fig. 3 shows the results of the electron density, N_e for $[(TeO_2)_{0.7}(B_2O_3)_{0.3}]_{1-x}(BaO)_x$ glass system. As shown in the figure, the trend in the graphs is similar to the Z_{eff} graph, which can be described in a similar Z_{eff} approach. At the low energy range E< 0.01 MeV the parameters Z_{eff} and N_{el} are similar and give maximum value where it depends of the photoelectric absorption. Over the intermediate region (0.05 MeV < E < 5 MeV) where Compton scattering prevails, the parameters decrease with energy. For high energies and around 100 MeV the parameters are constant, which attributes to the dominance of pair production. The same pattern result of Z_{eff} and N_e for energy range of 1 keV < E < 100 GeV were also observed by Agar *et al*. 2019 ($BaO–MoO_3–P_2O_5$) [19] and Abd-Allah *et al*., 2019 (*x* ZnO-(30-*x*) BaO-30PbO-40B_2O_3) [20].

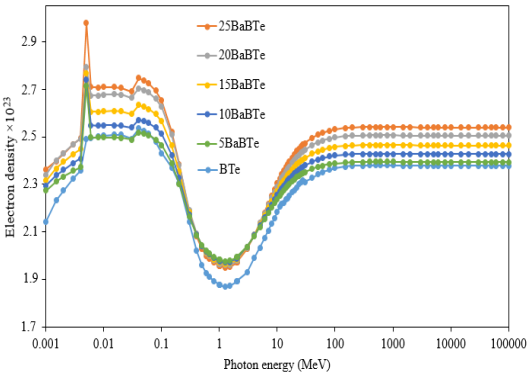

Fig. 3. Electron density, N_e *with different photon energies for* $[(TeO_2)_{0.7}(B_2O_3)_{0.3}]_{1-x}(BaO)_x$ *glass system.*

4. Conclusion

The results revealed that 25BaBTe glass sample with BaO of 0.25% mol among the studied samples is observed to have highest mass attenuation coefficient. The result from WinXCOM programme show that the change of effective atomic number (Z_{eff}) and electron density (N_e) in the energy range of 1 keV – 100 GeV are very related to the glass composition and photon energy. The interaction between photons and glass material are explained by photoelectric effect, Compton scattering and pair production mechanism.

Acknowledgement

The authors appreciate the financial support for this work from the Centre of Research Management & Innovation, National Defence University of Malaysia under grant no. UPNM/2019/GPJP/2/SG/6.

References

[1] K. Won-In, N. Sirikulrat, P. Dararutana, Advanced Materials Research **214**, 207 (2011).
[2] H. A. Saudi, S. U. El Kameesy, J. Phys.: Conf. Ser. **1253**, 012033 (2019).
[3] M. S. Al-Buriahi, C. Sriwunkum, H. Arslan, B. T. Tonguc, M. A. Bourham, Apply. Phys. A, **126**, 68 (2020).
[4] Y. Al-Hadeeth, M. I. Sayyed, S. A. Tijani, Nuclear Engineering and Technology **51**, 2005 (2019).
[5] M. K. Halimah, A. Azuraida, L. Hasnimulyati, M. Ishak, Journal of Non-Crystalline Solids **512**, 140 (2019).
[6] L. Gerward, N. Guilbert, K. B. Jensen, H. Levring, Radiat. Phys. Chem. **71**, 653 (2004).
[7] S. R. Manohara, S. M. Hanagodimath, K. S. Thind, L. Gerward, Nuclear Instruments and Methods in Physics Research B **266**(18), 3906 (2008).
[8] N. Kucuk, S. R. Manohara, S.M. Hanagodimath, L. Gerward, Radiation Physics and Chemistry **86**, 10 (2013).
[9] A. Un, F. Demir, Applied Radiation and Isotopes **653**, 73 (2013).
[10] V. P. Singh, M. E. Medhat, S. P. Shirmardi, Radiation Physics and Chemistry **106**, 255 (2015).
[11] D. K. Gaikwad, P. P. Pawara, T. P. Selvam, Radiation Physics and Chemistry **138**, 75 (2017).
[12] M. Esfandiari, S. P. Shirmardi, M. E. Medhat, Radiation Physics and Chemistry **99**, 30 (2014).
[13] A. Azuraida, M. K. Halimah, A. A. Sidek, C. A. C. Azurahanim, S. M. Iskandar, M. Ishak, A. Nurazlin, Chalcogenide Letters **12(10)**, 497 (2015).
[14] S. A. M. Issa, A. M. A. Mostafa, Journal of Alloys and Compounds **695**, 302 (2017).
[15] M. E. Çelikbilek, A. E. Ersundua, M. I. Sayyed, G. Lakshminarayana, S. Aydın, Journal of Alloys and Compounds **714**, 278 (2017).
[16] E. S. A. Waly, M. A. Fusco, M. A. Bourham, Annals of Nuclear Energy **96**, 26 (2016).
[17] A. Saeed, Y. H. Elbashar, R. M. Elshazly, Optical Quantum Electron **48**, 1 (2016).
[18] R. Polat, Z. Yalcin, O. Icelli, Nuclear Instruments and Methods in Physics Research A **629**, 185 (2011).
[19] O. Agar, M. I. Sayyed, H. O. TekinKawa, M. Kaky, S. O. Baki, I. Kity, Results in Physics **12**, 629 (2019).
[20] W. M. Abd-Allah, H. A. Saudi, K. S. Shaaban, Appl. Phys. A 125 (2019).